JACC Vol. 20, No. 1
July 1992:161–8



# Metabolic Evidence of Viable Myocardium in Regions With Reduced Wall Thickness and Absent Wall Thickening in Patients With Chronic Ischemic Left Ventricular Dysfunction

PASQUALE PERRONE-FILARDI, MD,* STEPHEN L. BACHARACH, PHD, VASKEN DILSIZIAN, MD, FACC, SIMONE MAUREA, MD, JOSE A. MARIN-NETO, MD, JAMES A. ARRIGHI, MD, JOSEPH A. FRANK, MD, ROBERT O. BONOW, MD, FACC

*Bethesda, Maryland*

**Reduced end-diastolic wall thickness with absent systolic wall thickening has been reported to represent nonviable myocardium in patients with chronic coronary artery disease. To assess whether reduced regional end-diastolic wall thickness and absent wall thickening accurately identify nonviable myocardium, 25 patients with ischemic left ventricular dysfunction (ejection fraction at rest 27 ± 10%) underwent positron emission tomography with oxygen-15–labeled water and $^{18}$fluorodeoxyglucose to assess metabolic activity and spin-echo gated nuclear magnetic resonance imaging to measure regional end-diastolic wall thickness and wall thickening. The presence of metabolic activity was defined as $^{18}$fluorodeoxyglucose uptake (corrected for partial volume) >50% of that in normal regions.**

**Of 355 myocardial regions evaluated, 266 were hypokinetic or normokinetic at rest and 89 were akinetic (that is, absent wall thickening). $^{18}$Fluorodeoxyglucose uptake was observed in 97% of the hypokinetic and normokinetic regions and in 74% of the akinetic regions. End-diastolic wall thickness was greater in akinetic regions with than in those without $^{18}$fluorodeoxyglucose uptake (11 ± 4 vs. 7 ± 3 mm, $p < 0.01$). The highest values for sensitivity and specificity of end-diastolic wall thickness in predicting the absence of metabolic activity in akinetic regions were 74% and 79%, respectively, and corresponded to an end-diastolic threshold of 8 mm. However, the positive predictive accuracy was only 55% and did not improve for other end-diastolic wall thickness values. In all myocardial regions, there was only a weak correlation between $^{18}$fluorodeoxyglucose activity and either end-diastolic wall thickness ($r = 0.17$) or wall thickening ($r = 0.32$).**

**Thus, metabolic activity is present in many regions with reduced end-diastolic wall thickness and absent wall thickening. These data indicate that assessment of regional anatomy and function may be inaccurate in distinguishing asynergic but viable myocardium from nonviable myocardium.**

***(J Am Coll Cardiol 1992;20:161–8)***

In patients with chronic coronary artery disease and left ventricular systolic dysfunction, regional myocardial asynergy at rest may result from either nonviable myocardium or viable but hypoperfused and dysfunctional myocardium (1,2). The distinction between these two conditions has relevant clinical implications because many asynergic yet viable myocardial regions recover function after coronary revascularization (3–5), leading to an increase in global left ventricular systolic function (3,4). In recent years, myocardial metabolic imaging with positron emission tomography has emerged as an accurate, noninvasive technique for distinguishing asynergic viable from nonviable myocardium in patients with coronary artery disease (4–6) and in predicting the recovery of regional and global left ventricular systolic function after revascularization (4,5). Nuclear magnetic resonance (NMR) imaging has also been reported (7,8) to identify nonviable myocardium in patients with chronic coronary artery disease, on the basis of presence of reduced regional wall thickness accompanied by lack of regional systolic wall thickening. Although NMR imaging provides better spatial resolution and image definition compared with positron emission tomography and allows the evaluation of regional systolic function, the accuracy of this approach in the differentiation between viable and nonviable myocardium has never been validated against established markers of myocardial viability, namely, the presence of metabolic activity or recovery of regional function after revascularization.

Thus, the purpose of the present study was to determine the ability of regional end-diastolic wall thickness and regional systolic wall thickening measurements to predict the presence or absence of regional metabolic activity in patients with chronic coronary artery disease and left ventricular dysfunction.

From the National Heart, Lung, and Blood Institute and the Clinical Center, National Institutes of Health, Bethesda, Maryland.

Manuscript received September 25, 1991; revised manuscript received January 6, 1992, accepted February 1, 1992.

*Current address: Division of Cardiology, University of Naples "Federico II", via Pansini 5, 80131, Naples, Italy.

Address for correspondence: Robert O. Bonow, MD, Cardiology Branch, National Heart, Lung, and Blood Institute, Building 10, Room 7B 15, 9000 Rockville Pike, Bethesda, Maryland 20892.



0735-1097/92/$5.00

## Methods

**Study patients.** We studied 25 patients (23 men and 2 women) with angiographically documented coronary artery disease (defined as the presence of ≥50% diameter stenosis in at least one major epicardial coronary artery) and left ventricular global systolic dysfunction. The mean age was 58 ± 9 years (range 38 to 78) and the mean radionuclide ejection fraction at rest was 27 ± 10% (range 10% to 47%). Thirteen of the 25 patients had triple-vessel and 7 patients had double-vessel coronary artery disease. Only one patient reported a history of diabetes mellitus. Fifteen of 25 patients reported a history of previous myocardial infarction, and the presence of pathologic Q waves on the electrocardiogram (ECG) was identified in an additional 4 patients. Twelve patients reported the occurrence of exertional angina and three patients had exertional dyspnea. Nine of the remaining 10 patients developed ECG signs of ischemia during exercise. All patients underwent equilibrium radionuclide angiography at rest and during exercise, positron emission tomography at rest after the administration of oxygen-15–labeled water ($H_2{}^{15}O$) and $^{18}$fluorodeoxyglucose, and gated NMR imaging at rest. In each patient, the positron emission tomographic and NMR studies were performed within a mean interval of 3 ± 3 days. All cardiac medications were withdrawn for ≥48 h in 21 patients. All patients gave informed written consent to the protocol, which was approved by the Institutional Human Research Committee in March 1989 (protocol # 86-H-209). The estimated radiation exposure did not exceed 0.78 rad total body dose.

**Radionuclide angiography.** Gated equilibrium radionuclide angiography was performed at rest and during bicycle exercise with the patient in the supine position using red blood cells labeled in vivo with 20 to 25 mCi of technetium-99m. Radionuclide angiography was performed a mean of 35 ± 55 days before the NMR study and within 37 ± 53 days of the positron emission study. High temporal resolution (20 ms/frame) time-activity curves were generated, from which the left ventricular ejection fraction was computed as previously described (9). Cardiac medications were discontinued for ≥48 h before the study in 20 of 25 patients. Ejection fraction during exercise did not increase in the group as a whole (from 27 ± 10% to 26 ± 13%) and it increased significantly (>5% increase) in only 4 of the 25 patients.

**Positron emission tomography.** Positron emission tomographic imaging was performed as previously described (10) to assess regional myocardial perfusion with $H_2{}^{15}O$ and exogenous glucose utilization with $^{18}$fluorodeoxyglucose, using a whole body positron emission tomographic camera producing 21 contiguous tomograms spaced 5.1 mm apart with a slice thickness of 13 mm and an in-plane reconstructed resolution of 6.5 mm. Images were obtained perpendicular to the long axis of the body to create a series of transaxial tomograms.

One hour before the $^{18}$fluorodeoxyglucose study, all patients received 50 g of oral glucose after an overnight fast. Two separate bolus injections of 12 to 15 mCi of $H_2{}^{15}O$ were administered intravenously 12 min apart, followed 15 min later by the administration of 5 mCi of $^{18}$fluorodeoxyglucose. Data were acquired for 5 min in list mode after each $H_2{}^{15}O$ injection and for 60 to 75 min in list mode after the $^{18}$fluoredeoxyglucose injection. The data beginning at 30 min after $^{18}$fluorodeoxyglucose injection, corresponding to the final 30 to 45 min of data acquisition, were reconstructed to create tomographic images of regional myocardial fluorodeoxyglucose uptake. To prevent movement artifacts, two seat belts were fastened around the patient's thorax during the acquisition of the positron study.

**Nuclear magnetic resonance imaging.** Electrocardiographic gated NMR imaging was performed using a 1.5 tesla scanner. A 15- to 20-min scan allowed acquisition of four to five slices at four to five noncontiguous time points in the cardiac cycle from end-diastole to end-systole using spin-echo imaging (echo time = 20 ms; repetition time = R wave to R wave time, two excitations). Each slice was 10 mm thick, with a center to center slice distance of 20 mm. Immediately after this acquisition, a second acquisition was begun, again consisting of four to five slices at four to five time points to fill in the gaps between slices. The final image sequence therefore consisted of 8 or 10 contiguous slices (10-mm thickness, 10-mm center to center interslice distance) at four to five time points in the cardiac cycle from end-diastole to end-systole. Total imaging time was 30 to 45 min. Images were acquired perpendicular to the body long axis and reconstructed as a series of transaxial tomograms to allow a direct comparison with the positron emission tomograms.

The time to end-systole was determined before NMR imaging from the left ventricular volume curve obtained from the radionuclide ventriculogram acquired at a similar heart rate (69 ± 12 beats/min for the radionuclide angiographic study and 72 ± 11 beats/min for the NMR study; mean difference between the studies 8 ± 6 beats/min). The intersequence delay of the NMR scan (that is, the time interval between successive time points) could then be adjusted so that the last (fourth or fifth) time point of the imaging scan occurred at end-systole as determined from the radionuclide angiographic study.

### *Data Analysis*

**Regional myocardial glucose uptake.** In each patient, five to six transaxial mid-ventricular tomograms from the $^{18}$fluorodeoxyglucose study were selected for the analysis. To objectively measure regional $^{18}$fluorodeoxyglucose activity, five myocardial regions of interest representing the posterolateral, anterolateral, anteroapical, anteroseptal and posteroseptal myocardium were drawn on each $^{18}$fluorodeoxyglucose tomogram. Regional $^{18}$fluorodeoxyglucose activity corrected for partial volume was then computed within each region of interest. In each patient, a "normal" myo-

cardial region was chosen and the $^{18}$fluorodeoxyglucose activity in all other regions was normalized to that of the normal reference region. The normal myocardial region in each of the 25 patients was chosen on the basis of the presence of normal blood flow (≥0.7 ml/g per min; mean 1 ± 0.23) (11–13) and normal systolic wall thickening at rest (4.3 ± 2.3 mm). Regional $^{18}$fluorodeoxyglucose activity >50% of that of the reference region was considered as evidence of metabolic activity (10,14). Myocardial regions showing $^{18}$fluorodeoxyglucose activity ≤50% of that of the reference region were interpreted as nonviable myocardium.

**Regional myocardial blood flow.** We computed absolute regional myocardial blood flow from the dynamic $H_2{}^{15}O$ data (15). The myocardial regions of interest previously constructed on the $^{18}$fluorodeoxyglucose images for measurement of regional $^{18}$fluorodeoxyglucose activity were applied to the tomographic $H_2{}^{15}O$ data to derive regional myocardial $H_2{}^{15}O$ time-activity curves. Absolute regional myocardial blood flow was calculated by fitting the myocardial $H_2{}^{15}O$ time-activity curve, M(t), to the formulation specified by Herrero et al. (16):

$$M(t) = (PV) \cdot F \cdot (LV(t) \times e^{-(F/p)t}) + (SO) \cdot LV(t),$$

where the variables of the fit are PV (a partial volume correction factor), F (flow in ml/g per min) and SO (a spillover correction factor, indicating the fraction of counts spilling from the left ventricular cavity into the myocardium); × is the convolution operation, which corrects for the fact that the injection was not a perfect bolus. The partition coefficient p was assumed fixed at 0.92, and the arterial input function LV(t) was measured directly by using the positron emission tomographic data from the left ventricular cavity (identified from the NMR imaging tomograms). Note that by fitting the data to this equation, one is able to simultaneously solve for all three unknown variables (that is, flow, spillover and partial volume recovery coefficient). This is similar to the method of previous investigators (11,12,16), except our fitting was weighted with the inverse variance of the data as determined from the total numbers of detected coincidences, dead time and correction for accidental coincidences.

This calculation also yields the recovery coefficient necessary to correct for partial volume effects. This recovery coefficient is valid not just for the $H_2{}^{15}O$ blood flow data, but also for the $^{18}$fluorodeoxyglucose data extracted from the same regions of interest, and was therefore used to correct both data sets.

**Regional myocardial wall thickness.** To assess regional end-diastolic wall thickness and absolute wall thickening, transaxial end-diastolic and end-systolic NMR images were analyzed by two independent operators unaware of the $^{18}$fluorodeoxyglucose results. The positron emission tomographic slices were aligned visually with the corresponding NMR slice by two observers unaware of the results with these two techniques with use of both the tomographic positron attenuation images and the positron emission images. In the positron attenuation images, anatomic reference points such as the lung outlines, the heart shadow and the slice in which the liver first begins to appear are clearly visible and could be matched with the corresponding structures in the NMR tomograms. Because of the different interslice distance (5.1 mm for positron emission tomography and 10 mm for NMR imaging), each NMR tomogram was matched to two contiguous positron emission tomograms. Because of the suboptimal visualization of inferior myocardium in the transaxial view and the troublesome measurements of wall thickening in the basal and apical tomograms, only mid-ventricular NMR tomograms were analyzed. An average of three NMR slices and six $^{18}$fluorodeoxyglucose tomographic planes were analyzed for each patient.

As just described, each positron emission tomographic slice had been divided into five regions of interest. By appropriate resampling, the positron emission tomographic and NMR images were made to be of identical size (that is, the same number of mm/pixel). The five regions of interest drawn on the positron emission tomogram could then be superimposed visually on the NMR image (with appropriate rotations and translations performed as needed). Because each region of interest encompassed a relatively large amount of myocardial tissue, minor misalignments obtained with this visual technique would not significantly alter the results. Thickness measurements were made at the center of each region of interest by manually identifying a point on the epicardial and endocardial borders perpendicular to the two surfaces. The length of the line segment joining these two points was calculated and taken as the wall thickness.

*Regional systolic wall thickening* was defined as the difference between end-systolic wall thickness and end-diastolic wall thickness. A total of 355 myocardial regions were evaluated, averaging 14 per patient. Myocardial regions were divided into three groups based on the extent of systolic wall thickening (17,18): 1) *akinetic or dyskinetic*, showing either absence of systolic wall thickening or systolic wall thinning; 2) *hypokinetic*, showing systolic wall thickening ≤2 mm; and 3) *normal*, showing systolic wall thickening >2 mm.

*Qualitative wall motion analysis by radionuclide angiography* was available in 22 of 25 patients. Wall motion abnormalities at rest were observed in 21 of these 22 patients, whereas impaired regional systolic wall thickening by NMR imaging was present in all 22 patients. Ten patients manifested abnormal wall motion in the lateral wall on radionuclide angiography, and in 9 of them regional systolic wall thickening by NMR imaging was abnormal in the corresponding territory. Similarly, radionuclide apical wall motion was abnormal in 20 patients, 18 of whom also manifested abnormal apical wall thickening. Finally, radionuclide septal wall motion was abnormal in 18 patients and in all of them abnormal septal wall thickening was observed.

**Statistical analysis.** Data are expressed as mean value ± SD. The two-tailed unpaired Student *t* test was applied for

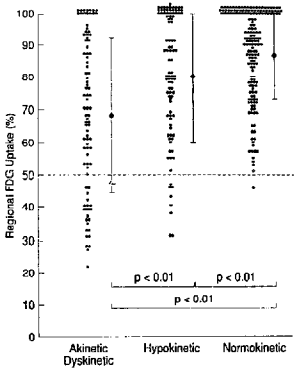


**Figure 1.** $^{18}$Fluorodeoxyglucose (FDG) uptake (expressed as a percent of normal activity) in relation to regional systolic function. Although akinetic and dyskinetic myocardial regions exhibited as a group reduced $^{18}$fluorodeoxyglucose uptake compared with hypokinetic and normokinetic myocardial regions, a large overlap was observed among the three groups.

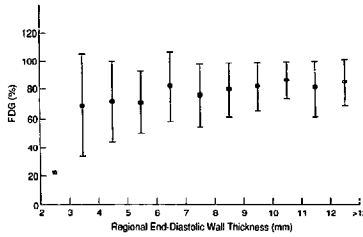


**Figure 2.** Relation between regional end-diastolic wall thickness and relative $^{18}$fluorodeoxyglucose (FDG) uptake (expressed as percent of a normal reference region) in all myocardial regions. Each point represents the mean (± 1 SD) $^{18}$fluorodeoxyglucose activity in all myocardial regions with the corresponding value of end-diastolic wall thickness. A large overlap is observed in the magnitude of $^{18}$fluorodeoxyglucose activity over the range of end-diastolic wall thickness.

comparisons between groups. A p value < 0.05 was accepted as the minimal level of significance.

## Results

**Regional wall thickness and blood flow in relation to systolic wall thickening.** Of the 355 myocardial regions evaluated, 89 showed akinesia or dyskinesia at rest (average regional systolic wall thickening −1.2 ± 1.8 mm); 95 myocardial regions were hypokinetic at rest (average systolic wall thickening 1.3 ± 0.5 mm), and in the remaining 171, systolic wall thickening was normal (4.2 ± 1.7 mm). Regional end-diastolic wall thickness did not differ significantly among the three groups of regions (10 ± 4, 10 ± 3 and 10 ± 3 mm, respectively); regional myocardial blood flow also did not differ (0.87 ± 0.34, 0.84 ± 0.34 and 0.9 ± 0.34 ml/g per min, respectively). Regional $^{18}$fluorodeoxyglucose uptake was significantly lower in the group of akinetic and dyskinetic regions compared with hypokinetic and normokinetic regions, although a large overlap among the three groups of regions was observed (Fig. 1). Among all myocardial regions, the correlation between regional $^{18}$fluorodeoxyglucose activity and either end-diastolic wall thickness (r = 0.17) (Fig. 2) or systolic wall thickening (r = 0.32) was poor. In particular, a significant positive linear correlation between regional $^{18}$fluorodeoxyglucose activity and regional end-diastolic wall thickness was found in 6 of the 25 patients and a significant positive linear correlation between regional $^{18}$fluorodeoxyglucose activity and regional systolic wall thickening was observed in 2 of the 25 patients.

**Metabolic activity in akinetic and dyskinetic myocardial regions.** Of the 89 myocardial regions showing akinesia or dyskinesia at rest, 66 (74%) had preserved metabolic activity (Fig. 1) as defined by the presence of regional $^{18}$fluorodeoxyglucose uptake by positron emission tomography. Asynergic myocardial regions showing evidence of metabolic activity were present in 24 (96%) of the 25 patients. Regional systolic wall thickening was similar between myocardial regions with and those without metabolic activity (−1.1 ± 1.7 vs. −1.1 ± 1.9 mm, respectively; p = NS). However, akinetic and dyskinetic regions with preserved metabolic activity showed greater end-diastolic wall thickness (11 ± 4 vs. 7 ± 3 mm; p < 0.001) and greater regional blood flow (0.90 ± 0.34 vs. 0.67 ± 0.34 ml/g per min; p < 0.05) than did regions without metabolic activity.

*The accuracy of regional end-diastolic wall thickness in predicting the presence or absence of metabolic activity in akinetic and dyskinetic myocardial regions* was then assessed for different values of end-diastolic thickness (Fig. 3) to determine the best combination of sensitivity and specificity. This cutoff value corresponded to an end-diastolic wall thickness of 8 mm. The sensitivity of an end-diastolic wall thickness <8 mm in predicting the absence of metabolic activity in akinetic or dyskinetic myocardial regions was 74% with a specificity of 79% (Fig. 3). However, although this cutoff value also yielded a very high negative predictive accuracy (90%), the positive predictive accuracy (that is, the ability of end-diastolic wall thickness <8 mm to predict the lack of metabolic activity in akinetic or dyskinetic regions) was only 55% (Fig. 3). Metabolic activity was present in 14 of 31 myocardial regions with an end-diastolic wall thickness <8 mm. Positive predictive accuracy did not considerably

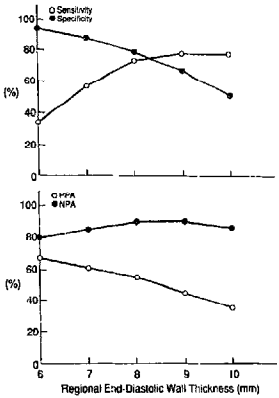


**Figure 3.** Sensitivity, specificity, positive predictive accuracy (PPA) and negative predictive accuracy (NPA) of different end-diastolic values in predicting the absence of metabolic activity in asynergic myocardial regions. For each end-diastolic wall thickness value, the positive predictive accuracy was defined as the ratio between the number of akinetic and dyskinetic segments without metabolic activity (true positive) and the number of akinetic segments with (false positive) and without (true positive) metabolic activity. Negative predictive accuracy was defined as the ratio between the number of akinetic and dyskinetic segments with metabolic activity (true negative) and the number of akinetic segments without (false negative) and with (true negative) metabolic activity. For the best combination of sensitivity and specificity (74% and 79%, respectively) corresponding to an end-diastolic wall thickness of 8 mm, the positive predictive accuracy is only 55%, indicating the presence of many asynergic regions with evidence of metabolic activity despite reduced wall thickness. Lower end-diastolic cutoff values did not significantly improve the positive predictive accuracy and did not result in a substantial decrease in sensitivity.

increase for lower cutoff values of end-diastolic wall thickness in which the sensitivity dramatically decreased (Fig. 3). Moreover, only a poor correlation was observed between $^{18}$fluorodeoxyglucose activity and end-diastolic wall thickness in regions with akinesia or dyskinesia ($r = 0.27$). An example of an akinetic myocardial region with reduced end-diastolic wall thickness but evidence of metabolic activity is illustrated in Figure 4.

**Metabolic activity in hypokinetic myocardial regions.** Of the 95 myocardial regions showing hypokinesia at rest, 87 (92%) had metabolic activity by positron emission tomography (Fig. 1). Twenty-eight myocardial regions (29%) in this group showed an end-diastolic wall thickness <8 mm; 21 of these manifested metabolic activity. The percent of regions with an end-diastolic wall thickness <8 mm was not significantly different from that observed in the group of akinetic and dyskinetic regions (Table 1). Regional $^{18}$fluorodeoxyglucose uptake (corrected for partial volume effects) did not differ significantly between hypokinetic regions with end-diastolic wall thickness <8 or ≥8 mm (Table 1). These values were also similar to those observed in akinetic and dyskinetic myocardial regions with an end-diastolic wall thickness ≥8 mm.

**Metabolic activity in myocardial regions with normal systolic wall thickening.** Of the 171 myocardial regions with normal systolic wall thickening, 170 (100%) demonstrated metabolic activity by positron emission tomography (Fig. 1). There were 42 myocardial regions (25%) in this group with an end-diastolic wall thickness <8 mm, 41 of which manifested the presence of metabolic activity. Again, no significant difference in the magnitude of $^{18}$fluorodeoxyglucose uptake was observed between myocardial regions with end-diastolic wall thickness <8 or ≥8 mm in this group (Table 1).

## Discussion

**Regional asynergy and viable myocardium.** Regional myocardial asynergy at rest may arise from either underlying *nonviable myocardium* or *dysfunctional yet viable myocardium* (1,2). As a consequence, the presence of even severe regional contraction abnormalities alone does not reliably indicate the presence of nonviable myocardium (19). In patients with chronic coronary artery disease, myocardial metabolic imaging with $^{18}$fluorodeoxyglucose has repeatedly demonstrated the presence of metabolic activity indicating viable myocardium in many regions showing severely impaired wall motion at rest (4,20,21). In addition, an improvement in regional systolic function after revascularization has been demonstrated by positron emission tomography in 78% to 85% of myocardial regions with preserved metabolic activity and impaired wall motion at rest (4,5) including many territories with severe hypokinesia or akinesia at rest (4). Thus, in the present study, the presence of metabolic activity, as defined by regional uptake of $^{18}$fluorodeoxyglucose, was considered as the reference gold standard for myocardial viability.

Metabolic activity was observed in 74% of the myocardial regions in which viability was at issue (that is, those exhibiting lack of systolic wall thickening). These data indicate that the majority of these territories have residual viable myocardium and are consistent with previous histopathologic (19), scintigraphic (22,23) and metabolic (24) studies showing the presence of viable myocardium in the majority of asynergic territories. Mean end-diastolic wall thickness in akinetic and dyskinetic regions was similar to that observed in hypokinetic and normokinetic regions. This finding can be explained by the fact that the group of akinetic and dyskinetic regions included areas of viable, presumably hibernating myocardium and areas of nonviable myocardium; asynergic but viable myocardium has been reported (19) to correspond histopathologically to only minimal muscle loss, whereas asynergic nonviable myocardium is associated with

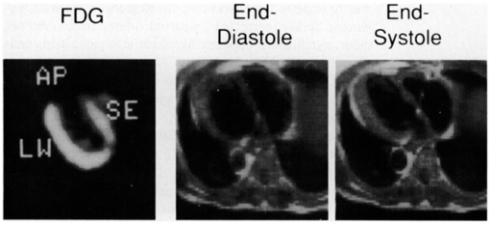


**Figure 4.** Matched positron emission tomographic study (**left**) and nuclear magnetic resonance imaging tomograms (**middle and right**) from a patient with a dilated left ventricle. Although the nuclear magnetic resonance images demonstrate reduced end-diastolic wall thickness with absent systolic wall thickening in the septum (SE), the positron emission tomogram shows $^{18}$fluorodeoxyglucose (FDG) uptake (and thus preserved metabolic activity) in the same territory, suggesting the presence of asynergic but viable myocardium. AP = apex; LW = lateral wall.

substantial muscle loss. This explanation appears consistent with the finding that akinetic and dyskinetic myocardial regions manifesting metabolic activity also showed as a group greater end-diastolic wall thickness than did regions without metabolic activity.

Previous clinical studies (7,8) also indicate that nonviable myocardial regions are associated with reduced end-diastolic wall thickness and lack of systolic wall thickening. Accordingly, we assessed the accuracy of different end-diastolic wall thickness values in predicting the presence or absence of metabolic activity in the myocardial regions exhibiting akinesia or dyskinesia. The best combination of sensitivity and specificity for predicting the absence of metabolic activity in these regions (74% and 79%, respectively) was achieved with a cutoff value of end-diastolic wall thickness of 8 mm (Fig. 3). The observed sensitivity was very similar to the 67% sensitivity for wall thinning assessed by NMR imaging in identifying areas of necrosis reported by Filipchuck et al. (25) in patients with coronary artery disease and previous myocardial infarction. However, the positive predictive accuracy was suboptimal despite reasonably good sensitivity, specificity and negative predictive accuracy. Thus, the probability of absent metabolic activity in an akinetic or dyskinetic myocardial region with an end-diastolic wall thickness <8 mm was only 55% (Fig. 3). Finally, in all myocardial regions only a very weak correlation was observed between the magnitude of $^{18}$fluorodeoxyglucose uptake and end-diastolic wall thickness (Fig. 2), which was also true when the same analysis was applied to regions with absent wall thickening. These findings clearly indicate the presence of viable myocardium in many akinetic or dyskinetic myocardial regions despite reduced wall thickness. The occurrence of viable myocardium in myocardial regions with reduced end-diastolic wall thickness was also confirmed by the observation that 25% of the myocardial regions showing normal systolic wall thickening had an end-diastolic wall thickness <8 mm (Table 1). Moreover, the magnitude of regional glucose uptake (after correction for the partial volume effect) was not significantly different between myocardial regions with an end-diastolic wall thickness <8 or ≥8 mm, both in myocardial regions with hypokinesia and in those with normal systolic wall thickening at rest (Table 1).

**Limitations.** In the present study, regional systolic wall thickening was measured at a single time point in the cardiac cycle, corresponding to global left ventricular end-systole as identified from radionuclide angiography. Thus, given the asynchrony of left ventricular contraction in patients with coronary artery disease and impaired left ventricular function, it is conceivable that some of the myocardial regions manifesting absence of wall thickening had prematurely completed their contraction or, conversely, had not reached maximal thickening when global left ventricular end-systole occurred.

To allow a direct comparison with the positron emission tomograms, NMR images were acquired in the transaxial plane perpendicular to the long axis of the body. Thus, the obliquity with the true cardiac long axis might introduce

**Table 1.** Regional End-Diastolic Wall Thickness and Relative $^{18}$Fluorodeoxyglucose Uptake in the Different Groups of Myocardial Regions

| | Regional Systolic Wall Thickening | | | | | |
|---|---|---|---|---|---|---|
| | Akinetic-Dyskinetic (n = 89) | | Hypokinetic (n = 95) | | Normal (n = 171) | |
| | EDT <8 mm (n = 31) | EDT ≥8 mm (n = 58) | EDT <8 mm (n = 28) | EDT ≥8 mm (n = 67) | EDT <8 mm (n = 42) | EDT ≥8 mm (n = 129) |
| FDG (%) | 56 ± 25 | 75 ± 21 | 75 ± 22 | 82 ± 19 | 87 ± 17 | 87 ± 14 |
| p Value | <0.001 | | NS | | NS | |

EDT = end-diastolic wall thickness; FDG = $^{18}$fluorodeoxyglucose (percent of normal activity).

some overestimation of regional myocardial wall thickness. However, the mean regional end-diastolic wall thickness values reported in the present study in the three groups of myocardial regions were similar to those reported by other investigators (26) using short-axis images. Conversely, acquisition of NMR imaging data in the short-axis plane has also been reported (27) to be suboptimal for the evaluation of regional systolic function in the presence of regional ischemia. Moreover, because absolute and not relative systolic wall thickening values were used in the present study, the potential inaccuracy in wall thickness measurements would have no effect on the regional wall thickening data. Finally, although image acquisition in the transaxial plane might lead to an overestimation of regional wall thickness, this effect would only strengthen the conclusion of the high frequency of metabolic activity in myocardial regions we identified to have both reduced wall thickness and reduced wall thickening.

As with all other techniques, motion of the left ventricular wall in and out of the imaging plane during the cardiac cycle was not considered. In addition, in the present study, the left ventricle was divided into five anatomic regions of interest. Although this procedure may be adequate in terms of the usually considered vascular territories, it is possible that some inhomogeneity of $^{18}$fluorodeoxyglucose or blood flow occurred within each region. In general, this would cause our results to be understated. Similarly, it should be remembered that the thickening measurements were obtained at one single representative point within each region.

In the present study, the presence of metabolic activity was arbitrarily defined as a relative $^{18}$fluorodeoxyglucose activity >50% of normal. In previous investigations (10,14) we demonstrated that myocardial regions with a reduction in $^{18}$fluorodeoxyglucose uptake >50% of normal correspond to severe irreversible thallium defects (10) and manifest absence of wall thickening (14), suggesting that they represent nonviable myocardium. Using the same cutoff value with regional thallium uptake, other investigators (23,28) demonstrated that the majority of myocardial regions with <50% of normal tracer uptake do not show improvement in function after revascularization, suggesting that such a cutoff may be employed to distinguish between viable and nonviable myocardium. In fact, the 50% cutoff used in the present study correctly predicted viability in 97% of the hypokinetic and normokinetic regions, which are by definition viable. In contrast, only 1 of 75 myocardial regions with $^{18}$fluorodeoxyglucose uptake <50% of normal showed normal wall thickening. In addition, the choice of different thresholds would not alter the conclusions of the study because of the widespread distribution of $^{18}$fluorodeoxyglucose activity values in the akinetic and dyskinetic myocardial regions (Fig. 1).

Finally, the functional outcome after revascularization of myocardium with absent systolic thickening but with preserved metabolic activity, especially in the presence of reduced end-diastolic wall thickness, cannot be predicted from the present study and needs to be evaluated. In addition, although asynergic myocardial regions with preserved metabolic activity were observed in all but one patient in this study, the mass of asynergic viable myocardium necessary for a clinically relevant improvement in global ventricular function after revascularization (and hence the number of patients who would potentially benefit from coronary revascularization) cannot be determined from our data. Moreover, because the study patients had stable chronic coronary artery disease and were in good hemodynamic condition, it is not known whether these findings can be extrapolated to the general population of patients with ischemic left ventricular dysfunction.

**Conclusions.** Our results demonstrate that metabolic activity is present in the majority of myocardial regions showing severe impairment of systolic function under rest conditions. Many of these territories might therefore exhibit improved function after revascularization. Although asynergic myocardial regions with absent metabolic activity are more likely to be thinner than those with preserved metabolic activity, reduced wall thickness with lack of systolic wall thickening is not always associated with nonviable myocardium. Thus, measures of regional left ventricular anatomy and function may be of limited value in distinguishing nonviable from asynergic viable myocardium in patients with chronic coronary artery disease and left ventricular dysfunction.

## References

1. Rahimtoola SH. The hibernating myocardium. Am Heart J 1989;117:211–21.
2. Braunwald E, Rutherford JD. Reversible ischemic left ventricular dysfunction: evidence for the "hibernating myocardium." J Am Coll Cardiol 1986;8:1467–70.
3. Rahimtoola SH. Coronary bypass surgery for chronic angina: 1981. Circulation 1982;65:225–41.
4. Tillisch J, Brunken R, Marshall R, et al. Reversibility of cardiac wall-motion abnormalities predicted by positron tomography. N Engl J Med 1986;314:884–8.
5. Tamaki N, Yonekura Y, Yamashita K, et al. Positron emission tomography using fluorine-18 deoxyglucose in evaluation of coronary artery bypass grafting. Am J Cardiol 1989;64:860–5.
6. Marshall RC, Tillisch JH, Phelps ME, et al. Identification and differentiation of resting myocardial ischemia and infarction in men with positron computed tomography, $^{18}$F-labeled fluorodeoxyglucose and N-13 ammonia. Circulation 1983;67:766–78.
7. Higgins CB, Lanzer P, Stark D, et al. Imaging by nuclear magnetic resonance in patients with chronic ischemic heart disease. Circulation 1984;69:523–31.
8. Higgins CB, McNamara MT. Magnetic resonance imaging of ischemic heart disease. Prog Cardiovasc Dis 1986;28:257–66.
9. Borer JS, Bacharach SL, Green MV, Kent KM, Epstein SE, Johnston GS. Real-time radionuclide cineangiography in the non-invasive assessment of global and regional left ventricular function at rest and during exercise in patients with coronary artery disease. N Engl J Med 1977;296:839–44.
10. Bonow RO, Dilsizian V, Cuocolo A, Bacharach SL. Myocardial viability in patients with chronic coronary artery disease and left ventricular dysfunction: thallium-201 reinjection versus $^{18}$F-fluorodeoxyglucose. Circulation 1991;83:26–37.
11. Iida H, Kanno I, Takahashi A, et al. Measurement of absolute myocardial blood flow with $H_2{}^{15}O$ and dynamic positron-emission tomography:

strategy for quantification in relation to the partial-volume effect. Circulation 1988;78:104–15.
12. Bergmann SR, Herrero P, Markham J, Weinheimer CJ, Walsh MN. Noninvasive quantitation of myocardial blood flow in human subjects with oxygen-15-labeled water and positron emission tomography. J Am Coll Cardiol 1989;14:639–52.
13. Gropler RJ, Siegel BA, Lee KJ, et al. Nonuniformity in myocardial accumulation of fluorine-18-fluorodeoxyglucose in normal fasted humans. J Nucl Med 1990;31:1749–56.
14. Perrone-Filardi P, Maurea M, Bacharach SL, et al. Does reduced regional fluorodeoxyglucose uptake with proportionate reduction in blood flow always indicate nonviable myocardium in coronary artery disease (abstr)? J Am Coll Cardiol 1991;17:121A.
15. Bacharach SL, Cuocolo A, Bonow RO, et al. Arterial blood concentration curves by cardiac PET without arterial sampling or image reconstruction. In: Computers in Cardiology 1988. Washington, DC: IEEE Computer Society Press, 1989:219.
16. Herrero P, Markham J, Bergmann SR. Quantitation of myocardial blood flow with $H_2{}^{15}O$ and positron emission tomography: assessment and error analysis of a mathematical approach. J Comput Assist Tomogr 1989;13: 862–73.
17. Sechtem U, Sommerhoff BA, Markiewicz W, White RD, Cheitlin MD, Higgins CB. Regional left ventricular wall thickening by magnetic resonance imaging: evaluation in normal persons and patients with global and regional dysfunction. Am J Cardiol 1987;59:145–51.
18. Higgins CB, Holt W, Pflugfelder P, Sechtem U. Functional evaluation of the heart with magnetic resonance imaging. Magn Reson Med 1988;6:121–39.
19. Bodenheimer MM, Banka VS, Hermann GA, Trout RG, Pasdar H, Helfant RH. Reversible asynergy: histopathologic and electrographic correlations in patients with coronary artery disease. Circulation 1976;53: 792–6.
20. Fudo T, Kambara H, Hashimoto T, et al. F-18 deoxyglucose and stress N-13 ammonia positron emission tomography in anterior wall healed myocardial infarction. Am J Cardiol 1988;61:1193–7.
21. Tamaki N, Yonekura Y, Yamashita K, et al. Relation of left ventricular perfusion and wall motion with metabolic activity in persistent defects on thallium-201 tomography in healed myocardial infarction. Am J Cardiol 1988;62:202–8.
22. Massie BM, Botvinick EH, Brundage BH, Greenberg B, Shames D, Gelberg H. Relationship of regional myocardial perfusion to segmental wall motion. Circulation 1978;58:1154–63.
23. Ragosta M, Beller GA, Watson DD, Kaul S, Gimple LW. Can resting thallium-201 imaging predict improvement in function after revascularization in patients with severely reduced LV function (abstr)? Circulation 1991;84(suppl II):II-89.
24. Brunken R, Tillisch J, Schwaiger M, et al. Regional perfusion, glucose metabolism, and wall motion in patients with chronic electrocardiographic Q wave infarctions: evidence for persistence of viable tissue in some infarct regions by positron emission tomography. Circulation 1986; 73:951–63.
25. Filipchuck NG, Peshock RM, Malloy CR, et al. Detection and localization of recent myocardial infarction by magnetic resonance imaging. Am J Cardiol 1986;58:214–9.
26. Peshock RM, Rokey R, Malloy CM, et al. Assessment of myocardial systolic wall thickening using nuclear magnetic resonance imaging. J Am Coll Cardiol 1989;14:653–9.
27. Beya R, Shapiro EP, Graves WL, et al. Quantification and validation of left ventricular wall thickening by a three-dimensional volume element magnetic resonance imaging approach. Circulation 1990;81:297–307.
28. Gibson RS, Watson DD, Taylor GJ, et al. Prospective assessment of regional myocardial perfusion before and after coronary revascularization surgery by quantitative thallium-201 scintigraphy. J Am Coll Cardiol 1983;3:804–15.